THE ASTROPHYSICAL JOURNAL, 491:181–190, 1997 December 10

COMPARISONS OF A GALACTIC KINEMATIC MODEL WITH TWO PROPER-MOTION SURVEYS IN THE VICINITY OF THE NORTH GALACTIC POLE

B. CHEN
Departament d'Astronomia i Meteorologia, Universitat de Barcelona, Avenida Diagonal 647, E-08028 Barcelona, Spain;
bchen@mizar.am.ub.es
Received 1997 February 17; accepted 1997 July 22

ABSTRACT

A Galactic kinematic model has been constructed for modeling the distributions of magnitude, colors, and proper motions. In addition, we have developed a star-count analysis algorithm, which uses all available information to extract Galactic structure parameters in an m-dimensional space of observables. In this paper, as a first application, we compare the predicted stellar distributions with two proper-motion surveys in the four-dimensional space of observables (V, $B-V$, μ_l, μ_b), thus discriminating between Galactic components on the basis of their magnitude, color, and kinematic distributions. Our result favors the existence of a velocity dispersion gradient from the Galactic plane for disk and thick-disk stars. The thick disk has a scale height of 1300 pc and a local density of 2.0% of the disk, and the scale height of the old disk is found to be about 340 pc. We find that a globular cluster function at the bright end of the spheroid luminosity function with an axial ratio (c/a) of 0.8 is in good agreement with the observations.

Subject headings: Galaxy: kinematics and dynamics — Galaxy: stellar content — Galaxy: structure — methods: data analysis — methods: statistical

1. INTRODUCTION

Over the last two decades, with high-efficiency, linear, two-dimensional detectors and fast measuring machines (PDS, COSMOS, MAMA), we have been able to derive high-quality data, including magnitudes, colors, and proper motions, over large areas of the sky. New and more accurate magnitude-limited surveys of colors and proper motions have been published (Chiu 1980; Spaenhauer 1989; Bienaymé et al. 1992; Soubiran 1992; Majewski 1992; Ojha et al. 1994a, 1994b; Spagna et al. 1996) or are being carried out. These multivariate star-count surveys, which contain valuable information about the Galaxy and its stellar components, allow us to separate well the different stellar populations and therefore strongly constrain their physical parameters.

Classical star-count analysis is used to infer the parameters of stellar populations by inverting the fundamental equation of stellar statistics. However, the inversion of the convolution integral is difficult because it is generally very ill-conditioned. Moreover, from the limited star-count observations, the individual distances of stars have to be derived by assuming that all the stars are on the main sequence, an assumption that has been criticized by Bahcall & Soneira (1984) and Ratnatunga (1988).

The second technique used by many investigators (Bahcall 1986; Robin & Crézé 1986b; Reid & Majewski 1993) is to test the consistency of a given model with the observations in the observational space. In this approach, star counts are used to derive physical parameters such as the scale heights of the disk and thick disk and the shape of the halo luminosity function (see Bahcall 1986 for a review).

It is now clear that photometric data alone cannot characterize the properties of the various components of the Galaxy (see, e.g., Gilmore, Reid, & Hewett 1985; Bahcall & Ratnatunga 1985). Kinematic data are required to compare the predictions of Galactic structure models with the observed trends in a multidimensional observational space (Gilmore, Wyse, & Kuijken 1989; Bienaymé et al. 1992).

In order to study a variety of kinematic samples from ground-based and space observations in the future, we have developed a Galactic kinematic model code and multivariate star-count analysis software (Chen et al. 1993; Chen 1996b). Samples simulated by means of the model code have been compared with observations in many Galactic directions. The intrinsic uncertainty due to the absorption (Sandage model) adopted in the Galactic model code can be significant at low and intermediate Galactic latitudes. For example, for the Bienaymé et al. (1992) proper-motion survey at intermediate Galactic latitude ($b = 47.^\circ3$) toward the Galactic center ($l = 2.^\circ7$), Bahcall-Soneira's Galactic model[1] and our model predict 1705 stars and 1683 stars, respectively, quite different from the real observation (1180 stars). Since we do not have good knowledge of the absorption, in this paper we analyze two star-count samples in the vicinity of the north Galactic pole, where the absorption is negligible.

There are two important differences between this study and previous works (Soubiran 1993; Majewski 1992; Reid & Majewski 1993). First, we compare the observed distributions with the model predictions in the space of observations, thus avoiding individual distance determinations, often a major source of error, and second, the comparison is performed in the four-dimensional space (V, $B-V$, μ_l, μ_b) simultaneously, including proper-motion distributions, providing good discrimination between stellar populations.

The rest of this paper is organized as follows: In § 2, we describe our Galactic kinematic model. In § 3, the star-count analysis algorithm is used to compare the model predictions with the observations. A discussion is presented in § 4.

2. GALACTIC KINEMATIC MODEL

We have constructed a Galactic kinematic model, which includes a disk, a thick disk, and a halo. The model can

[1] Available via anonymous ftp from the Institute for Advanced Study, School of Natural Sciences.

generate the simulated catalog according to the selection criteria used in the observation. In the simulated catalog, the observational variables (e.g., magnitudes, colors, proper motions, radial velocity) and the physical parameters (e.g., distance, absolute magnitude, metallicity, UVW velocities) for each star are known.

For disk stars, we have adopted the Robin & Crézé (1986a) Hess diagram. The stellar density laws used for the disk are exponential. The distribution of stars perpendicular to the plane of the Galaxy varies with luminosity (Bahcall & Soneira 1980). The old disk stars (with $M_V > 5.1$ mag) were assumed to have an exponential scale height of $H_{\max} = 300$ pc, and the young disk stars (with $M_V < 2.3$ mag) were taken to have a scale height of $H_{\min} = 90$ pc. For M_V between 2.3 and 5.1, the scale height was linearly interpolated between $H_{\min}$ and $H_{\max}$. The giant stars were assumed to have an exponential scale height of 250 pc. Our adopted velocity dispersions, asymmetric drift, and metallicity are the local values in the solar neighborhood. Because the variation of these parameters as a function of position in the Galaxy is not well determined, we have started by assuming their gradients to be zero.

The variation of the velocity dispersions with spectral type and luminosity class has been studied by many authors (Delhaye 1965; Wielen, Jahreiss, & Kruger 1983; Gómez et al. 1990). Following Mendez & van Altena (1996), we assigned the oldest stars a velocity dispersion $(\sigma_U, \sigma_V, \sigma_W) = (30, 20, 15)$ km s^{-1} and an asymmetric drift of -11 km s^{-1}. For young and intermediate disk stars, we assume velocity dispersions $(\sigma_U, \sigma_V, \sigma_W) = (15, 10, 10)$ and $(25, 15, 15)$ km s^{-1} and asymmetric drifts of -5 and -8 km s^{-1}, respectively (Chen et al. 1997). Recent work by Edvardsson et al. (1993) shows no detectable age-metallicity relationship over most of the duration of the old disk. They found a mean metallicity of -0.25 dex and metallicity dispersion of 0.2 dex for old disk stars. We have used their values in our Galactic model code.

Since the identification of the thick disk (Gilmore & Reid 1983), different approaches have been used to determine its physical parameters. The difficulty in measuring its characteristics lies in possible contamination of disk and halo stars. Different results in the literature are based on different stars selected using different techniques. Recently, we used principal component analysis to separate Galactic thick-disk stars from disk and halo in the four-dimensional space of magnitude, distance, spatial motions, and metallicity (Chen 1997). We found an asymmetric drift gradient for the thick disk, suggesting a dissipational settling as a mechanism for its formation. In this paper, we assume that the luminosity function of thick disk is similar to that of 47 Tuc. The H-R diagram is similar to that of the disk (Reid 1993). We adopt an asymmetric drift gradient of -14 ± 5 km s^{-1} kpc^{-1} and a drift velocity of the thick disk with respect to the LSR of -40 km s^{-1} at $Z = 0$ (Chen 1997). Wyse & Gilmore (1986) have found that the thick disk has a mean velocity dispersion $(\sigma_U, \sigma_V, \sigma_W) = (80, 60, 60)$ km s^{-1} and a scale height of 1500 pc; we have separated the Galactic thick disk from the disk and halo in the vicinity of the north Galactic pole (Chen 1997) and found that the thick disk has a mean velocity dispersion $(\sigma_U, \sigma_V) = (108, 63)$ km s^{-1}. In this investigation, as a first approximation we assume that the thick disk has a mean velocity dispersion $(\sigma_U, \sigma_V, \sigma_W) = (108, 63, 60)$ km s^{-1}. The scale height of the thick disk is 1500 pc, with a local density of 1.6% of the disk. Because we found the thick disk's metallicity to be the same as that of the old disk (Chen 1997), we assume a mean metallicity of -0.3 dex and metallicity dispersion of 0.30 dex for the thick disk. However, this parameter does not affect our analysis in this investigation in the four-dimensional space of $(V, B-V, \mu_l, \mu_b)$.

The halo luminosity function is assumed to be similar in shape to that of the disk for $M_V \geq 4$, but matching a globular cluster luminosity function at brighter magnitudes (Reid 1993). The color-magnitude diagram for both the main-sequence and evolved (red giant and horizontal branch) stars is based on the table given by Bergbush & VandenBerg (1992). The density law is adopted following de Vaucouleurs (1977). We adopt a halo-to-disk stellar density ratio in the solar neighborhood of 0.00150 and an axial ratio (c/a) of 0.9 (Yoshii, Ishida, & Stobie 1987); we assume a mean metallicity of -1.5 dex and metallicity dispersion of 0.76 dex for halo stars. Bahcall & Casertano (1986) have found the velocity ellipsoid of the halo to be (140, 100, 76) km s^{-1}, and this result has been confirmed by other investigations (Norris 1986; Morrison, Flynn, & Freeman 1990; Ryan & Norris 1991). From deep proper-motion surveys, Reid (1990), Majewski (1992), and Chen (1997) have found retrograde rotations of 35, 55, and 31 km s^{-1}, respectively. In this investigation, we assume a velocity ellipsoid for the halo of (138, 102, 85) km s^{-1} with a retrograde rotation $V_{\rm rot} = -31$ km s^{-1}.

Recently, Mendez & van Altena (1996) have derived the distance of the Sun from the Galactic plane, $Z = 2 \pm 34$ pc and $Z = -8 \pm 19$ pc, from two fields. We have adopted $Z = 0$ in our model. We have allowed for observational uncertainties by adding Gaussian errors to the V magnitude ($\epsilon_V = 0.05$ mag) and to the colors ($\epsilon_{B-V} = 0.08$ mag) of each "star" generated.

We should point out that these parameters in the model code are not the results of this investigation, but have been derived from previously published results. This model provides an interpretation of the observations, and such an interpretation is what we need in the first place to direct our later studies (§ 3) toward its improvement. Two stellar photometric and proper-motion surveys (Soubiran 1992; Majewski 1992) are investigated in this paper. Completeness limits, Galactic directions, areal coverage, and number of stars included in each survey are shown in Table 1. Detailed descriptions of the observations are given in the papers referred to above. In Figures 1 and 2, the model

TABLE 1

CHARACTERISTICS OF TWO PROPER-MOTION SURVEYS IN THE VICINITY OF THE NORTH GALACTIC POLE

Catalog	Author	Direction	Areal Coverage (deg^2)	Limiting Magnitude	Total Sample (stars)
M3.....	Soubiran 1992	$l = 58°$, $b = 80°$	7	$V = 17.5$	3450
SA 57.....	Majewski 1992	$l = 65°$, $b = 86°$	0.29	$V = 21.5$	250

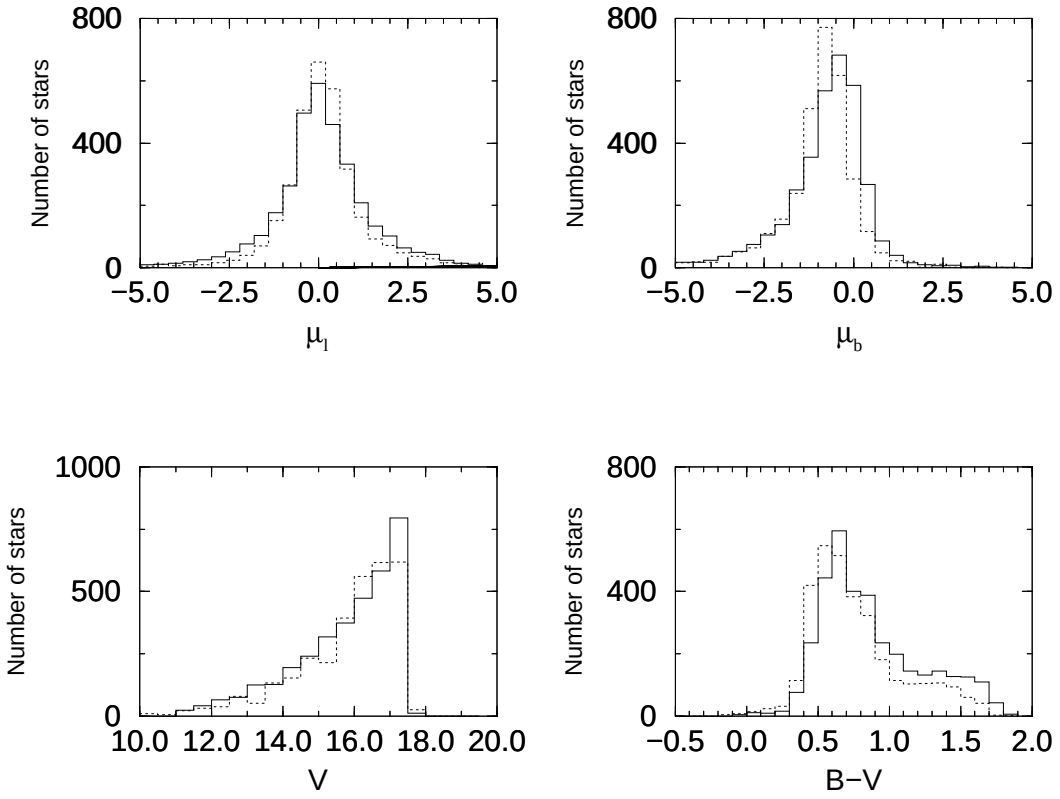

FIG. 1.—Predicted (*dotted histograms*) vs. observed (*solid histograms*) distributions for Soubiran's sample (M3)

predicted catalogs are compared with the real observations. One can see that such a model can basically represent the main characteristics of the observations. However, there are some significant disparities between the data and the model. For example, from the Soubiran data (hereafter "M3"), we found that the red side of the $B-V$ distribution cannot be well modeled, and for the Majewski data (hereafter "SA 57"), the model predicted too many stars between $V = 19$

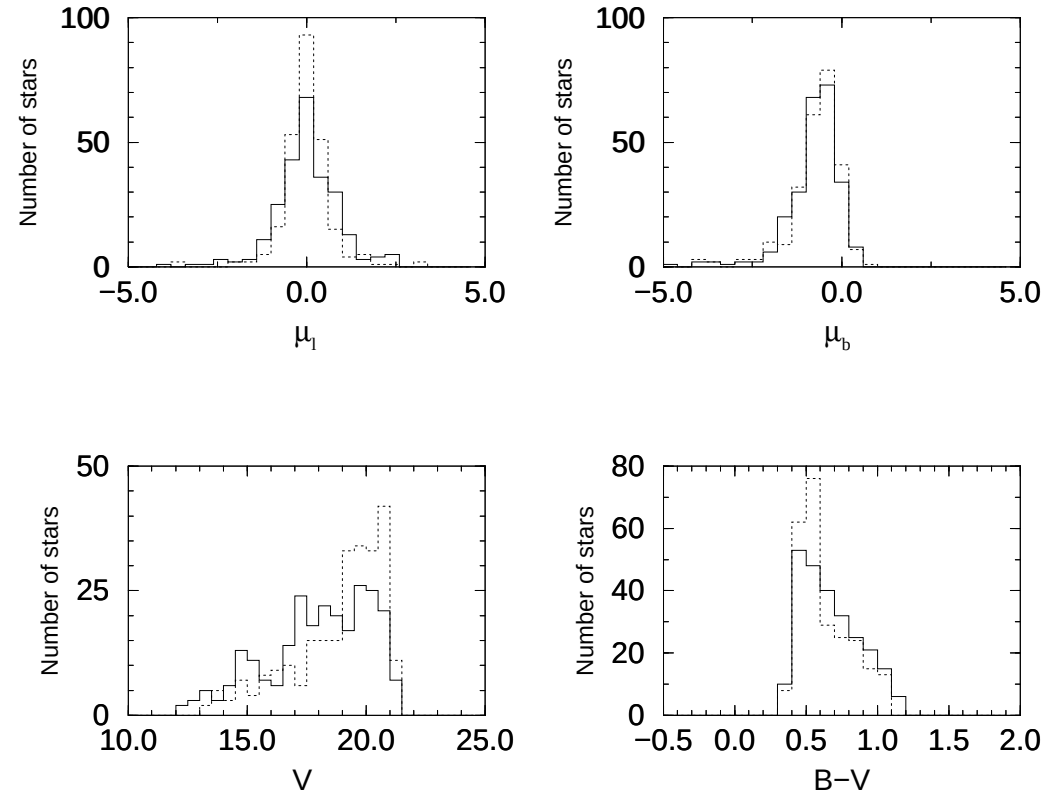

FIG. 2.—Same as Fig. 1, but for Majewski's sample (SA 57)

mag and $V = 21$ mag. We can also see some discrepancies in proper-motion distributions between the data and the model. In the following section (§ 3), we try to understand the cause of these disparities and improve the model parameters.

3. COMPARISONS OF THE MODEL WITH OBSERVATIONS

3.1. *Defining the Groups*

Galactic structure studies involve the manipulation of multivariate catalogs and their comparison with sophisticated synthesis models. The observational star counts are derived from a complete sample of stars in a certain region and brighter than a given apparent magnitude. Model simulated catalogs have been created according to the same selection criteria as the real star counts.

A numerical algorithm (Chen et al. 1993; Chen 1996b) for pattern recognition has been developed. It uses all available information—apparent magnitude, color, and proper motions—to extract Galactic structure parameters in an m-dimensional space of observables (V, $B-V$, μ_l, μ_b). The viability of the method has been tested by a series of Monte Carlo simulations. Results (Chen 1996b) show that the method is powerful.

Predefined groups should be defined in the simulated catalogs before the algorithm is applied. The groups can be formed from the stellar contents in the simulated sample and from the problems addressed.

With the M3 and the SA 57 samples in the vicinity of the north Galactic pole, we concentrated on discussing the kinematic gradients of stellar populations from the Galactic plane. Therefore, we have classified simulated stars into several groups according to their distance from Galactic plane for disk, thick-disk, and halo stars. Then we check the correlation coefficient in the space of observation, merge some groups that are strongly correlated, and obtain the final predefined groups. The means of the physical and observational parameters and their standard deviations (in parentheses) in each predefined group from the simulated M3 and SA 57 catalogs are shown in Tables 2 and 3, respectively.

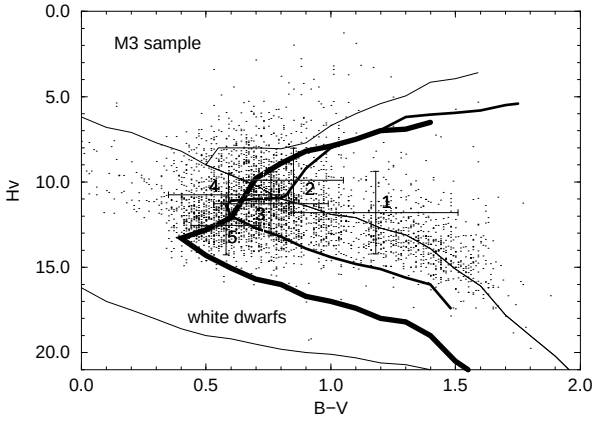

FIG. 3.—Reduced proper-motion diagram for Soubiran's star-count sample. Lines of different thickness indicate the ridge lines of the theoretical distributions for the disk, thick disk, and halo. Dots indicate the observed stars from the sample. The means and dispersions of the predefined groups have been overplotted.

The reduced proper-motion diagram, which combines photometric and proper-motion data, is useful to classify stellar populations (Chiu 1980; Dawson 1986). The reduced proper motion H_V was defined by Luyten (1922):

$$H_V = V + 5 \log \mu + 5 , \quad (1)$$

where μ is the total proper motion expressed in arcsec yr^{-1}. In Tables 2 and 3, the last column represents the means and standard deviations (in parentheses) of the reduced proper motion H_V in each group. In Figures 3 and 4, we show the means and dispersions of the predefined groups in the plane of the reduced proper motion and $B-V$ color. The lines of different thickness indicate the ridge lines of the theoretical distribution for the disk, thick disk, and halo derived by

TABLE 2

PARAMETERS FROM SIMULATED M3 SAMPLE

Group	Number of Stars	M_V	z (pc)	$B-V$	V	μ_l	μ_b	Comments	H_V
1	634	7.7 (1.9)	381 (157)	1.18 (0.33)	15.25 (1.6)	0.77 (3.7)	−1.16 (3.2)	Nearby disk stars	11.8 (2.42)
2	639	5.9 (1.2)	1006 (375)	0.85 (0.20)	15.59 (1.3)	0.19 (0.5)	−0.44 (0.6)	Remote disk stars	9.89 (1.87)
3	543	5.10 (1.53)	1681 (686)	0.76 (0.23)	15.60 (1.3)	0.11 (2.8)	−1.01 (2.3)	Nearby thick disk	11.28 (1.87)
4	591	3.52 (1.20)	4318 (1494)	0.59 (0.24)	16.26 (1.1)	−0.02 (0.4)	−0.65 (0.4)	Remote thick disk	10.75 (1.25)
5	748	4.58 (1.47)	4926 (3509)	0.58 (0.14)	16.63 (0.8)	−0.07 (1.5)	−1.45 (2.1)	Halo	12.54 (1.72)

NOTES.—Listed are the means and standard deviations (in parentheses) of physical and observational parameters in each predefined group from the simulated M3 catalog; μ_l and μ_b are proper motions expressed in arcseconds per 100 yr.

TABLE 3

PARAMETERS FROM SIMULATED SA 57 SAMPLE

Group	Number of Stars	M_V	z (pc)	$B-V$	V	μ_l	μ_b	Comments	H_V
1	26	5.7 (0.98)	997 (444)	0.78 (0.15)	15.8 (1.6)	0.27 (0.83)	−1.01 (0.77)	Old disk	10.24 (1.52)
2	74	5.3 (1.23)	4294 (2301)	0.76 (0.16)	18.1 (1.60)	0.11 (0.6)	−0.70 (0.5)	Thick disk	12.71 (1.81)
3	63	7.01 (1.39)	3843 (1493)	0.78 (0.20)	19.94 (1.4)	−0.23 (1.2)	−1.58 (2.0)	Nearby halo	16.15 (1.45)
4	97	5.2 (1.13)	10686 (5279)	0.54 (0.11)	19.95 (1.3)	−0.04 (0.4)	−0.56 (0.4)	Remote halo	14.25 (1.38)

NOTE.—Same as Table 2, but for the simulated SA 57 catalog.

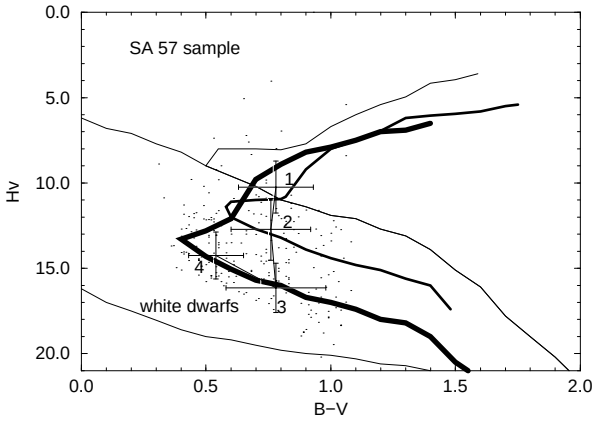

FIG. 4.—Same as Fig. 3, but for Majewski's star-count sample

Soubiran (1993). The dots indicate the observed stars from the M3 and the SA 57 samples, respectively.

We see that each physical group occupies a different position in the reduced proper-motion diagram, indicating that observations in the four-dimensional space (V, $B-V$, μ_l, μ_b) enable us to constrain the parameters of each stellar population.

3.2. *Multivariate Kernel Estimation*

Since this is the first application of our method, a simple description of the multivariate kernel estimation is necessary. The real stars are merged with model predicted stars in the m-dimensional space of observables. Each star in the merged sample is characterized by an m-dimensional vector $\boldsymbol{x}$. Suppose $p(\boldsymbol{x}\,|\,O)$ is the true probability density function (hereafter PDF) for the observed sample; then a multivariate kernel estimator $\hat{p}(\boldsymbol{x}\,|\,O)$ is given by

$$\hat{p}(\boldsymbol{x}\,|\,O) = \frac{1}{nh^m} \sum_{i=1}^{n} \frac{1}{|\boldsymbol{\Sigma}|^{1/2}(2\pi)^{m/2}} e^{-(\boldsymbol{x}-\boldsymbol{x}_i)^T \boldsymbol{\Sigma}^{-1}(\boldsymbol{x}-\boldsymbol{x}_i)/2h^2}, \quad (2)$$

where $\boldsymbol{x}$ is the point at which the estimate is being made, n is the number of stars in the observed sample, m is the dimension of the variables, $\boldsymbol{x}_i$ ($i = 1, \ldots, n$) is the observed sample set defined in m-dimensional space, $(\boldsymbol{x} - \boldsymbol{x}_i)^T$ is the transpose of the vector $(\boldsymbol{x} - \boldsymbol{x}_i)$, and $\boldsymbol{\Sigma}$ is the variance-covariance matrix of the observed sample.

The window width is denoted by h; an optimal window width derived by Silverman (1986) from minimizing the approximate mean integrated square error can be written as

$$h = \left(\frac{4}{m+2}\right)^{1/(m+4)} \sigma n^{-1/(m+4)}, \quad (3)$$

where σ is the average marginal variance, $\sigma^2 = m^{-1} \sum_{i=1}^{m} \sigma_i^2$.

From equation (2), for each star $\boldsymbol{x}$, we can also determine the PDF of each physical group ω_m in the simulated catalog, $\hat{p}(\boldsymbol{x}\,|\,\omega_m)$. In Table 4, we show these PDFs for the first 10 observed stars in the SA 57 sample. Column (1) represents the star number in the SA 57 sample. From column (2) to column (5), we list their observed variables ($B-V$, V, μ_l, μ_b), and from column (6) to column (9), the values of the PDF in each group $[\hat{p}(\boldsymbol{x}\,|\,\omega_m)]$ according to the model are given. The last column represents the values of PDF $[\hat{p}(\boldsymbol{x}\,|\,O)]$ for the observed sample at the point.

For example, the first star in Table 4 is a blue star. The derived values of the PDF in group 1 ($\omega_m = 1$) and group 2 ($\omega_m = 2$) are small; therefore, we can basically assign this star to the remote halo population, although membership in the nearby halo population is not ruled out. There is even a slight chance that the star belongs to the thick disk. Another remote halo population membership is star 3, with $V = 20.28$ and $B-V = 0.592$. On the another hand, star 5, with $V = 13.32$, is assigned as the disk population. In general, we can obtain only a probability that an observed star belongs to a particular group.

Suppose $\hat{p}(\omega_m)$ is the a priori probability density of ω_m. By Bayes's rules, the probability that a star $\boldsymbol{x}$ comes from group ω_m can be expressed as

$$p(\omega_m\,|\,\boldsymbol{x}) = C\hat{p}(\boldsymbol{x}\,|\,\omega_m)\hat{p}(\omega_m), \quad (4)$$

where C is a normalization constant.

3.3. *Kinematic Gradients from Galactic Plane*

The algorithm (Chen 1996b) should be used in an iterative approach. A first comparison of the multivariate den-

TABLE 4

PROBABILITY DENSITY FUNCTIONS FOR THE SA 57 SAMPLE

Object (1)	$B-V$ (2)	V (3)	μ_l (4)	μ_b (5)	$\hat{p}(\boldsymbol{x}\,\|\,1)$ (6)	$\hat{p}(\boldsymbol{x}\,\|\,2)$ (7)	$\hat{p}(\boldsymbol{x}\,\|\,3)$ (8)	$\hat{p}(\boldsymbol{x}\,\|\,4)$ (9)	$\hat{p}(\boldsymbol{x}\,\|\,O)$ (10)
1	0.403	18.13	−0.46	−1.25	0.0000	0.0003	0.0021	0.0043	0.0060
2	0.704	16.81	−0.12	−0.29	0.0036	0.0064	0.0000	0.0006	0.0056
3	0.592	20.28	−0.27	−0.87	0.0000	0.0033	0.0020	0.0229	0.0238
4	0.870	15.20	0.09	−0.76	0.0010	0.0018	0.0000	0.0001	0.0019
5	0.626	13.32	−0.41	−1.03	0.0002	0.0000	0.0000	0.0000	0.0010
6	0.505	16.46	0.17	−0.95	0.0003	0.0035	0.0005	0.0006	0.0085
7	0.773	16.97	1.82	−0.57	0.0001	0.0001	0.0000	0.0000	0.0008
8	0.652	17.51	−0.52	0.01	0.0004	0.0023	0.0000	0.0002	0.0035
9	0.616	18.02	0.74	−0.30	0.0001	0.0025	0.0003	0.0021	0.0051
10.....	0.416	17.85	0.15	−0.80	0.0000	0.0013	0.0013	0.0034	0.0100

NOTES.—Listed are the PDFs for the first 10 observed objects in the Majewski sample (SA 57). Col. (1) represents the star number in the SA 57 sample. From col. (2) to col. (5), we list the observed variables ($B-V$, V, μ_l, μ_b); μ_l and μ_b are proper motions expressed in arcseconds per 100 yr. From col. (6) to col. (9), the values of the PDF in each group $[\hat{p}(\boldsymbol{x}\,|\,\omega_m)]$ according to the model are given. The last column represents the values of the PDF $[\hat{p}(\boldsymbol{x}\,|\,O)]$ for the observed sample at the point.

TABLE 5

MODEL PREDICTIONS AND OBSERVATIONS FOR THE M3 SAMPLE

Quantity	Group 1	Group 2	Group 3	Group 4	Group 5
$\overline{V}_{\rm model}$	15.25 (1.6)	15.59 (1.3)	15.60 (1.3)	16.26 (1.1)	16.63 (0.8)
$\overline{V}_{\rm data}$	15.30 ± 0.06	15.66 ± 0.05	15.61 ± 0.05	16.27 ± 0.05	16.43 ± 0.05
	(1.7 ± 0.04)	(1.4 ± 0.04)	(1.3 ± 0.04)	(1.1 ± 0.04)	(1.1 ± 0.04)
$\overline{B-V}_{\rm model}$	1.18 (0.3)	0.85 (0.2)	0.76 (0.2)	0.59 (0.2)	0.58 (0.1)
$\overline{B-V}_{\rm data}$	1.20 ± 0.01	0.85 ± 0.01	0.77 ± 0.01	0.61 ± 0.01	0.60 ± 0.01
	(0.4 ± 0.01)	(0.2 ± 0.01)	(0.3 ± 0.01)	(0.3 ± 0.01)	(0.2 ± 0.01)
$(\overline{\mu_l})_{\rm model}$	0.77 (3.7)	0.19 (0.5)	0.11 (2.8)	−0.02 (0.4)	−0.07 (1.6)
$(\overline{\mu_l})_{\rm data}$	0.68 ± 0.13	0.12 ± 0.04	0.17 ± 0.10	0.03 ± 0.04	0.10 ± 0.09
	(3.8 ± 0.09)	(0.9 ± 0.03)	(2.5 ± 0.07)	(0.8 ± 0.03)	(1.7 ± 0.06)
$(\overline{\mu_b})_{\rm model}$	−1.16 (3.2)	−0.44 (0.6)	−1.01 (2.3)	−0.65 (0.4)	−1.45 (2.1)
$(\overline{\mu_b})_{\rm data}$	−1.31 ± 0.09	−0.55 ± 0.02	−0.92 ± 0.09	−0.61 ± 0.04	−1.28 ± 0.12
	(3.1 ± 0.06)	(0.9 ± 0.01)	(2.0 ± 0.06)	(0.7 ± 0.03)	(2.3 ± 0.09)

NOTES.—Comparison of the group characteristics between the model predictions and the observations from the M3 sample. Listed are the barycenters and dispersions (in parentheses) of real and simulated samples in each predefined group. The model was constructed by assuming velocity dispersion gradients from the Galactic plane for the disk and thick disk to be zero.

sities of the model (this section) with the data allows us to detect significant systematic shifts between the group characteristics and the observed distributions. Then, applying these shifts to the model, the same computation allows us to measure the relative density of each physical group (see § 3.4).

The posterior probability $\hat{p}(\omega_m \mid \boldsymbol{x}_i)$ derived in equation (4) is used to derive weighted means and the covariance matrix for each group from the observed data as follows:

$$\overline{X_l^{\omega_m}} = \frac{\sum_{i=1}^{n} \hat{p}(\omega_m \mid \boldsymbol{x}_i) x_{il}}{\sum_{i=1}^{n} \hat{p}(\omega_m \mid \boldsymbol{x}_i)}, \tag{5}$$

$$\sigma_{lj}^{\omega_m 2} = \frac{\sum_{i=1}^{n} \hat{p}(\omega_m \mid \boldsymbol{x}_i)(x_{il} - x_l)(x_{ij} - x_j)}{\sum_{i=1}^{n} \hat{p}(\omega_m \mid \boldsymbol{x}_i)}, \tag{6}$$

where l and j are two axes of the multidimensional space and x_{il} indicates the ith star with its lth variable in the observed catalog. Equations (5) and (6) describe the statistical properties of observed stars in each predefined group. In Tables 5 and 6, we show the barycenters and dispersions of real and simulated samples in each predefined group for M3 and SA 57, respectively.

Because the samples used are in the vicinity of the north Galactic pole, μ_l and μ_b provide information about eventual radial motions (U component) and about the rotation of the different populations (V component), respectively. We compare these barycenters and variances between the real sample and the model simulated sample. The disagreements are interpreted as erroneous physical properties of the model groups.

In the M3 field (Table 5), the predicted proper-motion dispersions (σ_{μ_l}, σ_{μ_b}) of group 1 stars agree with those observed. However, the proper-motion dispersions predicted for group 2 are smaller than observed; the same applies to the group 1 stars in SA 57 (Table 6). These differences can be attributed to an increase of velocity dispersion with distance from the Galactic plane for disk stars. This effect was predicted by Fuchs & Wielen (1987); accordingly, a new model that incorporates their velocity dispersion gradients was constructed.

For the thick disk, from the M3 data, we found that the predicted proper-motion dispersions in group 3 (nearby thick disk) are slightly higher than the observed dispersions and that the predicted proper-motion dispersions in group 4 (remote thick disk) are smaller than those observed. This is a clear indication of an increase in velocity dispersion with distance from the Galactic plane, because a change in the thick-disk asymmetric drift mainly affects the median proper motions but not the proper-motion dispersions. Spaenhauer (1989) found a gradient in V-velocity dispersion of $\partial\sigma_V/\partial z \sim 37$ km s^{-1} kpc^{-1} up to $\sim$3 kpc. However, Majewski found a smaller gradient of $\partial\sigma_V/\partial z \sim 12$ km s^{-1} kpc^{-1} after separating the thick-disk stars from the halo

TABLE 6

MODEL PREDICTIONS AND OBSERVATIONS FOR THE SA 57 SAMPLE

Quantity	Group 1	Group 2	Group 3	Group 4
$\overline{V}_{\rm model}$	15.76 (1.6)	18.07 (1.6)	19.94 (1.4)	19.95 (1.3)
$\overline{V}_{\rm data}$	15.61 ± 0.23	17.46 ± 0.20	18.65 ± 0.22	19.47 ± 0.16
	(1.7 ± 0.16)	(1.5 ± 0.14)	(1.4 ± 0.16)	(1.6 ± 0.11)
$\overline{B-V}_{\rm model}$	0.78 (0.1)	0.76 (0.2)	0.78 (0.2)	0.54 (0.1)
$\overline{B-V}_{\rm data}$	0.79 ± 0.02	0.76 ± 0.03	0.68 ± 0.03	0.54 ± 0.01
	(0.2 ± 0.01)	(0.2 ± 0.02)	(0.2 ± 0.02)	(0.1 ± 0.01)
$(\overline{\mu_l})_{\rm model}$	0.27 (0.8)	0.11 (0.6)	−0.23 (1.2)	−0.04 (0.4)
$(\overline{\mu_l})_{\rm data}$	−0.11 ± 0.21	0.22 ± 0.13	−0.30 ± 0.16	0.00 ± 0.05
	(1.6 ± 0.15)	(1.0 ± 0.09)	(1.1 ± 0.11)	(0.4 ± 0.04)
$(\overline{\mu_b})_{\rm model}$	−1.01 (0.8)	−0.70 (0.5)	−1.58 (2.0)	−0.56 (0.4)
$(\overline{\mu_b})_{\rm data}$	−0.81 ± 0.14	−0.95 ± 0.10	−1.26 ± 0.15	−0.52 ± 0.04
	(1.5 ± 0.10)	(0.7 ± 0.08)	(2.1 ± 0.11)	(0.4 ± 0.03)

NOTE.—Same as Table 5, but for the SA 57 sample.

TABLE 7

MODEL PREDICTIONS AND OBSERVATIONS FOR THE M3 SAMPLE INCLUDING A VELOCITY DISPERSION GRADIENT

Quantity	Group 1	Group 2	Group 3	Group 4	Group 5
$\overline{V}_{\rm model}$	15.34 (1.6)	15.78 (1.2)	15.80 (1.2)	16.23 (1.1)	16.52 (0.8)
$\overline{V}_{\rm data}$	15.33 ± 0.06	15.77 ± 0.05	15.76 ± 0.05	16.17 ± 0.05	16.40 ± 0.05
	(1.7 ± 0.04)	(1.3 ± 0.04)	(1.3 ± 0.04)	(1.2 ± 0.04)	(1.0 ± 0.04)
$\overline{B-V}_{\rm model}$	1.16 (0.3)	0.87 (0.2)	0.75 (0.2)	0.55 (0.2)	0.57 (0.1)
$\overline{B-V}_{\rm data}$	1.17 ± 0.01	0.85 ± 0.01	0.75 ± 0.01	0.62 ± 0.01	0.60 ± 0.01
	(0.4 ± 0.01)	(0.2 ± 0.01)	(0.3 ± 0.01)	(0.3 ± 0.01)	(0.2 ± 0.01)
$(\overline{\mu_l})_{\rm model}$	0.79 (3.8)	0.17 (0.9)	0.15 (2.6)	−0.05 (0.7)	−0.08 (1.6)
$(\overline{\mu_l})_{\rm data}$	0.74 ± 0.13	0.16 ± 0.04	0.13 ± 0.11	0.01 ± 0.04	0.03 ± 0.08
	(3.8 ± 0.08)	(1.0 ± 0.04)	(2.6 ± 0.08)	(0.8 ± 0.04)	(1.6 ± 0.06)
$(\overline{\mu_b})_{\rm model}$	−1.24 (3.3)	−0.50 (1.0)	−1.10 (2.1)	−0.71 (0.8)	−1.37 (2.2)
$(\overline{\mu_b})_{\rm data}$	−1.28 ± 0.08	−0.57 ± 0.03	−0.97 ± 0.09	−0.65 ± 0.05	−1.30 ± 0.12
	(3.2 ± 0.06)	(1.0 ± 0.01)	(2.2 ± 0.06)	(0.9 ± 0.03)	(2.2 ± 0.09)

NOTE.—Same as Table 5, but constructed assuming an increase in velocity dispersion with distance from the Galactic plane for the disk and thick disk.

TABLE 8

MODEL PREDICTIONS AND OBSERVATIONS FOR THE SA 57 SAMPLE INCLUDING A VELOCITY DISPERSION GRADIENT

Quantity	Group 1	Group 2	Group 3	Group 4
$\overline{V}_{\rm model}$	15.81 (1.6)	18.11 (1.6)	19.90 (1.3)	19.99 (1.3)
$\overline{V}_{\rm data}$	15.67 ± 0.21	17.53 ± 0.20	18.68 ± 0.25	19.53 ± 0.18
	(1.7 ± 0.14)	(1.6 ± 0.14)	(1.4 ± 0.13)	(1.5 ± 0.11)
$\overline{B-V}_{\rm model}$	0.73 (0.1)	0.71 (0.2)	0.75 (0.2)	0.53 (0.1)
$\overline{B-V}_{\rm data}$	0.75 ± 0.02	0.73 ± 0.03	0.69 ± 0.03	0.51 ± 0.01
	(0.2 ± 0.01)	(0.2 ± 0.02)	(0.2 ± 0.02)	(0.1 ± 0.01)
$(\overline{\mu_l})_{\rm model}$	0.29 (1.5)	0.13 (1.1)	−0.28 (1.2)	−0.09 (0.4)
$(\overline{\mu_l})_{\rm data}$	−0.07 ± 0.21	0.24 ± 0.13	−0.37 ± 0.15	0.07 ± 0.05
	(1.6 ± 0.15)	(1.0 ± 0.13)	(1.2 ± 0.12)	(0.4 ± 0.05)
$(\overline{\mu_b})_{\rm model}$	−1.07 (1.7)	−0.73 (0.8)	−1.64 (2.1)	−0.59 (0.4)
$(\overline{\mu_b})_{\rm data}$	−0.92 ± 0.14	−0.94 ± 0.10	−1.32 ± 0.15	−0.57 ± 0.04
	(1.6 ± 0.12)	(0.9 ± 0.09)	(2.2 ± 0.11)	(0.4 ± 0.04)

NOTE.—Same as Table 7, but for the SA 57 sample.

stars. We have adopted our results (Chen 1997) of $\partial\sigma_V/\partial z = 30$ km s^{-1} kpc^{-1} and $\partial\sigma_V/\partial z = 15$ km s^{-1} kpc^{-1} and local velocity dispersions ($Z = 0$) of $(\sigma_U, \sigma_V) = (40, 30)$ km s^{-1} in the new model.

For Galactic halo, from Table 5 (group 5) and Table 6 (groups 3 and 4), we did not find a significant discrepancy in proper motions between the predicted distribution and the observed one. However, the predicted magnitudes (V) are significantly fainter than observed. We will discuss this below (§ 3.4).

In Tables 7 and 8, we present results from the M3 and SA 57 fields after adoption of the velocity dispersion gradients mentioned earlier. We can see a marked improvement in the agreement between the observed and predicted proper-motion dispersions.

3.4. *Galactic Structure at the North Galactic Pole*

To fit the model parameters to the data, we assume that the contributions of observed stars at each point of the m-dimensional space can be fitted by a linear combination of the contributions of the model groups. Let α_{ω_m} be the coefficient to apply to group ω_m in order to fit the data:

$$\sum \alpha_{\omega_m} \hat{p}(\boldsymbol{x} \mid \omega_m) = \hat{p}(\boldsymbol{x} \mid O) \, . \tag{7}$$

This equation must be valid at each point $\boldsymbol{x}$, leading to a system of n equations, where n is the total number of stars in the catalog.

TABLE 9

RESULTS FROM LEAST-SQUARES SOLUTION FOR THE M3 SAMPLE

	Group 1	Group 2	Group 3	Group 4	Group 5
Group 1.....	0.02				
Group 2.....	−0.45	0.02			
Group 3.....	0.23	−0.78	0.03		
Group 4.....	−0.03	0.29	−0.59	0.02	
Group 5.....	−0.01	−0.13	0.27	−0.83	0.05
α_{ω_m}	1.30	1.51	1.22	0.62	0.85

NOTES.—The estimated parameters are shown in the bottom line of the matrix. The values on-diagonal are the errors on the estimated coefficients (ϵ_{ω_m}), and the values off-diagonal give the correlation coefficients between the groups.

Tables 9 and 10 show the least-squares solutions from the two samples. The estimated parameters—the ratio of the number of stars in the observed data to the model for each group—are shown in the bottom line of each matrix. If α_{ω_m}

TABLE 10

RESULTS FROM LEAST-SQUARES SOLUTION FOR THE SA 57 SAMPLE

	Group 1	Group 2	Group 3	Group 4
Group 1.....	0.11			
Group 2.....	−0.53	0.09		
Group 3.....	0.14	−0.38	0.06	
Group 4.....	0.05	−0.08	−0.39	0.05
α_{ω_m}	1.46	0.94	0.77	0.45

NOTE.—See notes to Table 9.

TABLE 11

RESULTS FROM LEAST-SQUARES SOLUTION FOR THE M3 SAMPLE WITH IMPROVED PARAMETERS

	Group 1	Group 2	Group 3	Group 4	Group 5
Group 1.....	0.04				
Group 2.....	−0.34	0.02			
Group 3.....	0.19	−0.84	0.03		
Group 4.....	−0.03	0.41	−0.71	0.03	
Group 5.....	−0.01	−0.30	0.56	−0.83	0.02
α_{ω_m}	0.93	1.03	0.91	0.99	1.05

NOTES.—Same as Table 9, but using the improved model parameters. The new model was constructed by improving Galactic structure parameters (see § 3.4).

is greater than 1, the model cannot predict enough stars in group ω_m; in contrast, if α_{ω_m} is smaller than 1, the model predicts too many stars. The values on-diagonal are the errors of the estimated coefficients; the values off-diagonal give the correlation coefficient between the groups. For M3 sample, the derived coefficients have smaller error bars, because there are more stars in this catalog than that in the SA 57 sample.

TABLE 12

RESULTS FROM LEAST-SQUARES SOLUTION FOR THE SA 57 SAMPLE WITH IMPROVED PARAMETERS

	Group 1	Group 2	Group 3	Group 4
Group 1.....	0.13			
Group 2.....	−0.49	0.10		
Group 3.....	0.12	−0.32	0.05	
Group 4.....	0.03	−0.06	−0.39	0.06
α_{ω_m}	1.15	1.10	0.93	0.89

NOTE.—See notes to Table 11.

In the M3 field, the model predicts too few disk stars (by 30% for group 1 and 51% for group 2); in the SA 58 field, it predicts too few (by 46%) group 1 stars. Therefore, new models were tested by increasing the old disk scale height.

For the thick disk, from the SA 57 sample (group 2), the total numbers predicted by the model are comparable to the observations. However, from the M3 data (groups 3 and 4), we found that too few thick-disk stars were predicted in the nearby group (by 22%), while too many were predicted in the remote group (by 38%).

For halo stars, from the M3 data (group 5), the model predicts too many halo stars (by 15%), and from the SA 57 data, we have also found that model predicts too many halo stars in groups 4 and 5, by 23% and 55%, respectively. In the previous section, we noted that the predicted apparent magnitudes for halo stars are fainter than observed. Both results favor a smaller axial ratio, which will steepen the density law toward the pole and reduce the predicted number of halo stars. Therefore, instead of an axial ratio (c/a) of 0.9, a smaller value has been tested in our new model.

New models were generated by improving the disk scale height, thick disk scale height and local density, and axial ratio of halo stars. For each model, the predicted catalogs are compared with the observations. An iterative procedure is carried out until the final model, with all $|\alpha_{\omega_m} - 1| \leq 3\sigma$ for the SA 57 and the M3 samples.

Finally, we adopt an old disk scale height of 340 pc, a thick-disk scale height of 1300 pc and a local density of 2%

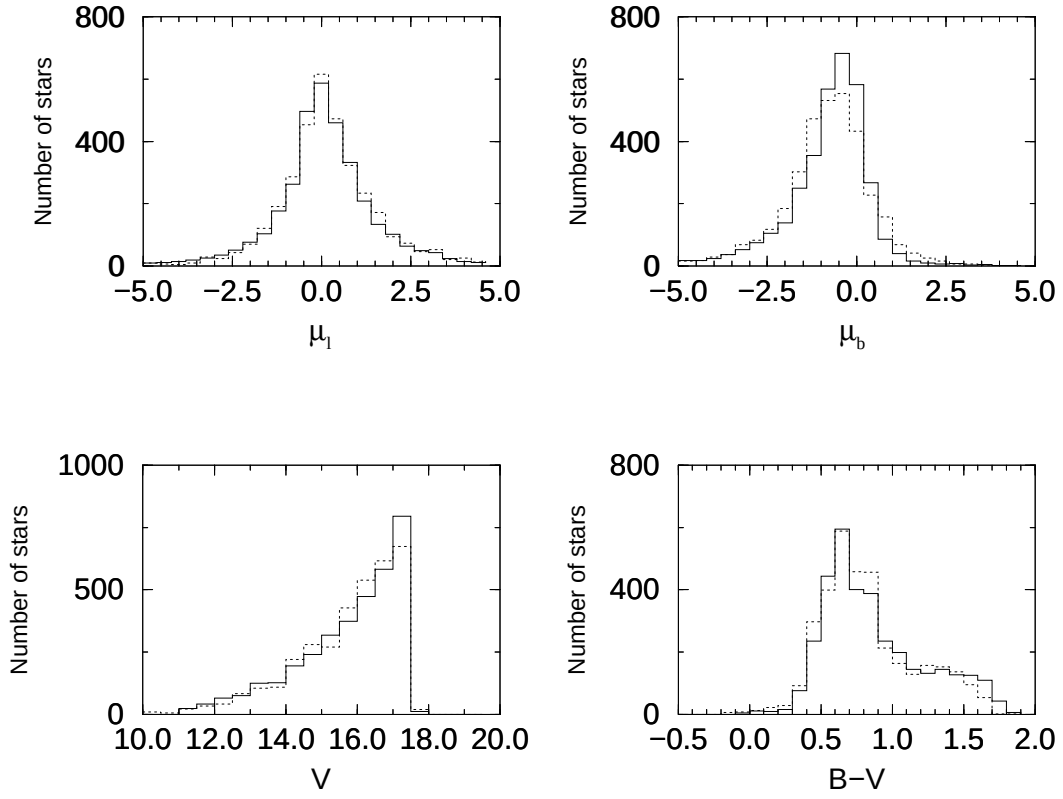

FIG. 5.—New-model predicted (*dotted line*) vs. observed (*solid line*) distributions for Soubiran's sample. The new model was constructed by improving kinematic and structural parameters.

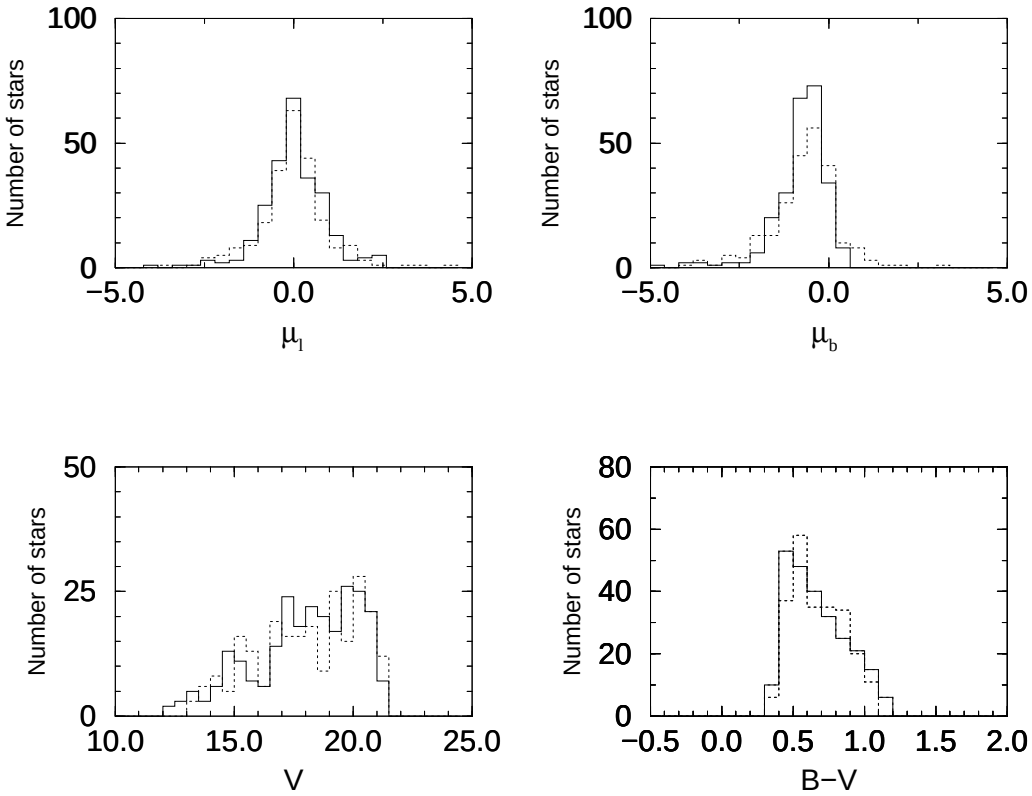

FIG. 6.—Same as Fig. 5, but for Majewski's sample

for the disk stars, and an axial ratio of 0.8. In Tables 11 and 12, we show the least-squares results for the M3 data and the SA 57 data obtained using these new model parameters. We can see that these parameters in Galactic structure are very similar to the original values suggested by Gilmore & Reid (1983) and our previous results (Chen 1996a). In Figures 5 and 6, new model predicted catalogs are compared with the real observations, and one can see an improvement in the agreement between the observed and the predicted distributions.

4. DISCUSSION

In this paper, we have constructed a Galactic kinematic model that can model the distributions of magnitude, colors, proper motions, and radial velocity. The predicted stellar distributions are compared with the observations in the four-dimensional space of observables (V, $B-V$, μ_l, μ_b) simultaneously, thus discriminating between Galactic components on the basis of their magnitude, color, and kinematic distributions. A numerical algorithm (Chen 1996b) for pattern recognition has been used to investigate the intrinsic stellar distributions of each population and to constrain the Galactic model parameters.

We have analyzed two stellar photometric and proper-motion surveys in the vicinity of the north Galactic pole. Our result favors the existence of velocity dispersion gradients from the Galactic plane, suggested by Fuchs & Wielen (1987) for disk stars. This result has also been derived by Mendez & van Altena (1996) at low Galactic latitude. We find that the scale height of the old disk is about 340 pc. This is slightly larger than Reid's result of 325 pc (Reid 1993). However, Gould, Bahcall, & Maoz (1993) found an excess of faint disk stars from the *Hubble Space Telescope* (*HST*) Snapshot Survey and suggested that perhaps the scale height for faint disk stars was greater than 325 pc for bright stars. For the Galactic thick disk, we found clear indication of an increase in velocity dispersions with distance from the Galactic plane. Spaenhauer (1989) and Majewski (1992) found gradients in velocity dispersion from classical star-count analysis. We have confirmed our previous results (Chen 1997) from a reanalysis of Majewski's star-count data in the four-dimensional space of (U, V, [Fe/H], Z) and found that the gradients $\partial\sigma_V/\partial z = 30$ km s^{-1} kpc^{-1} and $\partial\sigma_V/\partial z = 15$ km s^{-1} kpc^{-1} and local velocity dispersions ($Z = 0$) of $(\sigma_U, \sigma_V) = (40, 30)$ km s^{-1} are in good agreement with the observed proper-motion distributions. The thick disk has a scale height of 1300 pc, and the local normalization is 2.0% that of the old disk. These results may help us to understand the mechanism of the thick-disk formation. Our results favors a dissipational settling as the main mechanism for the formation of the thick disk. However, there could have been a later heating event in the disk, such as a major merger by satellite accretion as described by Quinn, Hernquist, & Fullager (1992). We did not find significant kinematic gradients for Galactic halo. Comparisons of the model predictions with observations show that a globular cluster function at the bright end of the spheroid luminosity function with an axial ratio (c/a) of 0.8 is in good agreement with the observations.

The Guide Star Catalog (GSC-II) is the only project currently planned to produce an all-sky catalog of stars with colors, magnitudes, positions, and proper motions from *HST* observations (Lasker et al. 1995). We plan to use our Galactic model and our star-count analysis algorithm to constrain the main stellar populations of the Galaxy from ground-based and space observations in the future.

I thank Michel Crézé, who motivated me to use multivariate data analysis to interpret proper-motion surveys and gave me many useful suggestions and comments; without his help, this work would not have been possible. Many thanks to A. C. Robin, J. Torra, and the referee for their thoughtful and constructive comments on this manuscript. This work was supported by the Generalitat de Catalunya (PIEC), CICYT, under contract ESP 91-1133-E and by DGICYT under contract PB 91-0857.

REFERENCES

Bahcall, J. N. 1986, ARA&A, 24, 577
Bahcall, J. N., & Casertano, S. 1986, ApJ, 308, 347
Bahcall, J. N., & Ratnatunga, K. U. 1985, MNRAS, 213, 39
Bahcall, J. N., & Soneira, R. M. 1980, ApJS, 47, 357
———. 1984, ApJS, 55, 67
Bergbush, P. A., & VandenBerg, D. A. 1992, ApJS, 81, 163
Bienaymé, O., Mohan, V., Crézé, M., Considère, S., & Robin, A. C. 1992, A&A, 253, 389
Chen, B. 1996a, A&A, 306, 733
———. 1996b, A&AS, 118, 181
———. 1997, AJ, 113, 311
Chen, B., Asiain, R., Figueras, F., & Torra, J. 1997, A&A, 318, 29
Chen, B., Crézé, M., Robin, A. C., & Bienaymé, O. 1993, in ASP Conf. Ser. 52, Astronomical Data Analysis Software and Systems II, ed. R. J. Hanish, R. J. V. Brissenden, & J. Barnes (San Francisco: ASP), 489
Chiu, L. T. G. 1980, ApJS, 44, 31
Dawson, P. C. 1986, ApJ, 311, 984
Delhaye, J. 1965, in Galactic Structure, ed. A. Blaauw & M. Schmidt (Chicago: Univ. Chicago Press), 61
de Vaucouleurs, G. 1977, AJ, 82, 456
Edvardsson, B., Andersen, J., Gustafsson, B., Lambert, D. L., Nissen, P. E., & Tomkin, J. 1993, A&A, 275, 101
Fuchs, B., & Wielen, R. 1987, in The Galaxy, ed. G. Gilmore & B. Carswell (NATO ASI Ser. C, 207) (Dordrecht: Reidel), 375
Gilmore, G., & Reid, N. 1983, MNRAS, 202, 1025
Gilmore, G., Reid, N., & Hewett, P. 1985, MNRAS, 213, 257
Gilmore, G., Wyse, R. F. G., & Kuijken, K. 1989, ARA&A, 27, 555
Gómez, A. E., Delhaye, J., Grenier, S., Jaschek, C., Arenou, F., & Jaschek, M. 1990, A&A, 236, 95
Gould, A., Bahcall, J. N., & Maoz, D. 1993, ApJS, 88, 53
Lasker, B. M., McLean, B. J., Jenkner, H., Lattanzi, M. G., & Spagna, A. 1995, in Future Possibilities for Astrometry in Space, ed. F. van Leeuven & M. A. C. Perryman (ESA SP-379) (Noordwijk: ESA), 137
Luyten, W. J. 1922, On the Relation between Parallax, Proper Motion, and Apparent Magnitude (Lick Obs. Bull. 336) (Berkeley: Univ. California Press)
Majewski, S. R. 1992, ApJS, 78, 87
Mendez, R. A., & van Altena, W. F. 1996, AJ, 112, 655
Morrison, H. L., Flynn, C., & Freeman, K. C. 1990, AJ, 100, 1191
Norris, J. 1986, ApJS, 61, 667
Ojha, D. K., Bienaymé, O., Robin, A. C., & Mohan, V. 1994a, A&A, 284, 810
———. 1994b, A&A, 290, 771
Quinn, P. J., Hernquist, L., & Fullager, D. P. 1992, ApJ, 403, 74
Ratnatunga, K. U. 1988, AJ, 93, 1132
Reid, I. N. 1990, MNRAS, 247, 70
———. 1993, in ASP Conf. Ser. 49, Galaxy Evolution: The Milky Way Perspective, ed. S. R. Majewski (San Francisco: ASP), 37
Reid, N., & Majewski, S. R. 1993, ApJ, 409, 635
Robin, A. C., & Crézé, M. 1986a, A&A, 157, 71
———. 1986b, A&AS, 64, 53
Ryan, S. G., & Norris, J. E. 1991, AJ, 101, 1835
Silverman, B. W. 1986, Density Estimation for Statistics and Data Analysis (London: Chapman & Hall)
Soubiran, C. 1992, A&A, 259, 394
———. 1993, A&A, 274, 181
Spaenhauer, A. 1989, in The Gravitational Force Perpendicular to the Galactic Plane, ed. A. G. Davis Philip & P. K. Lu (Schenectady: L. Davis Press), 45
Spagna, A., Lattanzi, M. G., Lasker, B. M., McLean, B. J., Massone, G., & Lanteri, L. 1996, A&A, 311, 758
Wielen, R., Jahreiss, H., & Kruger, R. 1983, in IAU Colloq. 76, The Nearby Stars and the Stellar Luminosity Function, ed. A. G. Davis Philip & A. R. Upgren (Schenectady: L. Davis Press), 163
Wyse, R. G., & Gilmore, G. F. 1986, AJ, 91, 855
Yoshii, Y., Ishida, K., & Stobie, R. S. 1987, AJ, 93, 323